

Cubic Splines and Fourier Series Approach to Study Temperature Variation in Dermal Layers of Elliptical Shaped Human Limbs

Mamta Agrawal, Neeru Adlakha, and K.R. Pardasani

Abstract—An attempt has been made to develop a seminumerical model to study temperature variations in dermal layers of human limbs. The model has been developed for two dimensional steady state case. The human limb has been assumed to have elliptical cross section. The dermal region has been divided into three natural layers namely epidermis, dermis and subdermal tissues. The model incorporates the effect of important physiological parameters like blood mass flow rate, metabolic heat generation, and thermal conductivity of the tissues. The outer surface of the limb is exposed to the environment and it is assumed that heat loss takes place at the outer surface by conduction, convection, radiation, and evaporation. The temperature of inner core of the limb also varies at the lower atmospheric temperature. Appropriate boundary conditions have been framed based on the physical conditions of the problem. Cubic splines approach has been employed along radial direction and Fourier series along angular direction to obtain the solution. The numerical results have been computed for different values of eccentricity resembling with the elliptic cross section of the human limbs. The numerical results have been used to obtain the temperature profile and to study the relationships among the various physiological parameters.

Keywords—Blood Mass Flow Rate, Metabolic Heat Generation, Fourier Series, Cubic splines and Thermal Conductivity.

I. INTRODUCTION

THE skin in human body or animal body is boundary lamina, which plays an important role in temperature regulation. It is composed of three layers namely epidermis, dermis, and subcutaneous tissues (see Fig. 1). There are no blood vessels in the epidermis, so there is no blood flow and metabolic activity in this outermost layer. The density of the blood vessels increases as we go down the dermis and becomes almost uniform in the layer below the dermis namely subdermal tissues. A human body maintains its body core temperature at a uniform temperature under the normal atmospheric conditions.

M. Agrawal is Research Scholar with the Department of Mathematics Maulana Azad National Institute of Technology, Bhopal-51, INDIA, (e-mail: mamta_agrawal2311@yahoo.co.in)

N. Adlakha is Faculty of the Department of Mathematics Jaypee Institute of Technology, Guna, Ragogarh, (e-mail: neeru.adlakha@jiet.ac.in)

K.R. Pardasani is Head of the Department of Mathematics, Maulana Azad National Institute of Technology, Bhopal-51, INDIA, phone: 9425027637; fax: +91755-2670562;

(e-mail: kamalraj@rediffmail.com; kamalraj@hotmail.com)

In order to maintain this core temperature parameters like rate of blood mass flow, rate of metabolic heat generation and thermal conductivity vary in response to changes in atmospheric conditions. However, in extreme parts of a human body the core temperature is not uniform at low atmospheric temperature, where the core temperature of limbs varies extensively as we move away from the body core. This may be because the arterial blood has cooled down while travelling towards the extremities. The heat flow in in-vivo tissues is given by W.Perl [1] as given below.

$$\rho \cdot \bar{c} \cdot \frac{\partial T}{\partial t} = \text{Div.}(K \cdot \text{grad} T) + m_b \cdot c_b (T_A - T) + S. \quad (1)$$

Here ρ , \bar{c} , K , and S are respectively the density, specific heat, thermal conductivity, and rate of metabolic heat generation in tissues. m_b , c_b , and T_A are the blood mass flow rate, specific heat of the blood, and arterial blood temperature respectively. Perl [1], used this equation to find temperature distribution in tissue medium. Patterson [2], made an attempt for experimental determination of temperature profiles in Skin and Subcutaneous Tissues (SST) region. Saxena and Arya [3], developed a three layered *finite element* model to find the temperature profiles in SST region for a one dimensional steady state case. Saxena and Bindra [4], and Pardasani and Saxena [5], used analytical and numerical techniques to obtain temperature profiles in the SST region for one dimensional steady state case. Pardasani and Adlakha [6], investigated this problem for a two dimensional steady case in skin and subcutaneous tissues (SST). Later Saxena and Pardasani [7], and Pardasani and Adlakha [8], have extended this approach in SST region involving tumors. In [9], an analytical model to predict temperature levels as a function of time in human legs during cooling has been developed. Saxena and Bindra [10], developed a pseudo analytic approach to study the problem of heat flow in human limbs for a two-dimensional steady state case. This approach consists of *Ritz method* and *Fourier series*. Pardasani and Adlakha [11], further developed and extended this approach to study temperature distribution in annular tissue layers of a human, or animal body using *Cubic splines* approach and *Fourier series* [12], for circular region. Saxena and Gupta [13], also developed this approach to study

the problem of heat flow in human limbs. Pardasani and Jas [14], studied heat flow in limbs for a three dimensional steady state case by using *seminumerical techniques*. Pardasani and Shakya [15], [16] also extended finite element modeling to infinite domains.

In this problem a two-dimensional *elliptical region* resembling with the cross-section of a human limb is considered. Each layer has different physical and physiological properties. A *cubic splines* interpolation has been employed for radial direction while for the angular direction the *Fourier series* has been used due to uniformity in each annular subregion. The outer layer is assumed to be exposed to the environment and heat loss takes place due to convection, radiation, and evaporation. The inner most part is assumed to be at a known variable temperature which is possible when one side of inner cross section consists of major blood vessels.

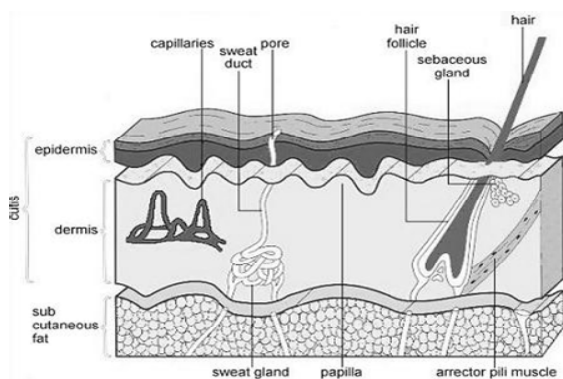


Fig. 1 Composition of skin layers

II. MATHEMATICAL MODEL

Equation (1) in elliptical coordinates for a two dimensional steady state case may be written as:

$$\frac{1}{D} \left[K \cdot \frac{\partial}{\partial \mu} \left(\frac{\partial T}{\partial \mu} \right) + K \cdot \frac{\partial}{\partial \nu} \left(\frac{\partial T}{\partial \nu} \right) \right] + M(T_A - T) + S = 0. \quad (2)$$

Here, $D = d^2(\sinh^2 \mu + \sin^2 \nu)$, (μ, ν) are elliptic coordinates and d is taken as *eccentricity* of elliptical shape. The boundary conditions imposed are as follows:

$$-K \cdot \frac{\partial T}{\partial \eta} \Big|_{\mu = \mu_N} = h(T - T_a) + L \cdot E \quad (3)$$

$$\text{And } T(\mu_0, \nu) = F(\nu). \quad (4)$$

Here h is the heat transfer coefficient T_a is atmospheric temperature, L , and E are respectively the latent heat, and rate of sweat evaporation. Also $\frac{\partial T}{\partial \eta}$ is the partial derivative of T along the normal to the surface, and $F(\nu)$ is some known function.

Now, the region is divided into N layers with inner and outer distances equal to μ_0 and μ_N respectively (see Fig. 2).

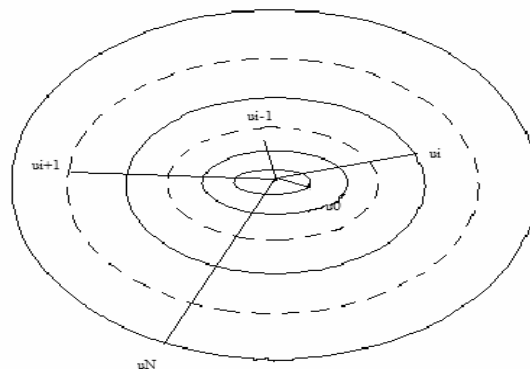


Fig. 2 Elliptical Cross-section of a human limb divided in to N -layers

Equation (2) for each layer may be written as:

$$K_i \cdot \frac{\partial^2 T^{(i)}}{\partial \mu^2} + K_i \cdot \frac{\partial^2 T^{(i)}}{\partial \nu^2} + A_1^{(i)} \cdot M_i(T_A^{(i)} - T^{(i)}) + A_1^{(i)} \cdot S_i = 0 \quad (5)$$

Where, $A_1^{(i)} = d_i^2(\sinh^2 \mu_i + \sin^2 \nu_i)$, $d_i =$ *eccentricity* of each layer.

The outer boundary condition (3) may be written as;

$$K_i \cdot \frac{\partial T^{(i)}}{\partial \eta} \Big|_{\mu = \mu_N} = h(T_i - T_a) + L \cdot E, \text{ where } i = N \text{ only.} \quad (6)$$

Let T_i and D_i ($i = 0$ (1) N) denote respectively the values of T and second order derivative of T at the distance μ_i ($i = 0$ (1) N) from the centre. The *cubic spline* function $T^{(i)}$ [12], in the i^{th} layer is written as:

$$T^{(i)}(\mu) = \frac{(\mu_i - \mu)^3}{6 \cdot \Delta_i} \cdot D_{i-1} + \frac{(\mu - \mu_{i-1})^3}{6 \cdot \Delta_i} \cdot D_i + C_1 \cdot \mu + C_2 \quad \text{for } i = 1(I) N. \quad (7)$$

Here C_1 and C_2 are constants, which are determined by using the conditions, $T^{(i)}(\mu_i) = T_i$ and $T^{(i)}(\mu_{i-1}) = T_{i-1}$

The following assumptions have been made for each subregion.

$$K^{(i)}(\mu_i) = K_i, M^{(i)}(\mu_i) = M_i, \text{ and } S^{(i)}(\mu_i) = S_i \text{ for } i = 0(I) N$$

$$T_A^{(i)} = \sigma_1^{(i)} \cdot T_{i-1} + \sigma_2^{(i)} \cdot T_0, \text{ where } \sigma_1^{(i)} = 1 - \sigma_2^{(i)},$$

$$\sigma_2^{(i)} = \frac{\mu_0}{\mu_{i-1}} \text{ for } i = 1(I) N \quad (8)$$

Now, the first order left-hand and right-hand derivatives of $T(\mu)$ at the node μ_i are given by

$$T^{(i)}(\mu_i^-, \nu) = \frac{\Delta_i}{6} \cdot D_{i-1} + \frac{\Delta_i}{3} \cdot D_i + \frac{T_i - T_{i-1}}{\Delta_i} \quad \text{for } i = 1(I) N. \quad (9)$$

$$T^{(i+1)}(\mu_i, \nu) = \frac{-\Delta_{i+1}}{3} \cdot D_i - \frac{\Delta_{i+1}}{6} \cdot D_{i+1} + \frac{T_{i+1} - T_i}{\Delta_{i+1}}$$

for $i=0(1)N-1$. (10)

Where, $T' = \frac{\partial T}{\partial \mu}$ and $D_i = \frac{\partial^2 T_i}{\partial \mu^2}$

Also,

$$K_i(\mu_i, \nu) \cdot T^{(i)}(\mu_i) = K_{i+1}(\mu_i, \nu) \cdot T^{(i+1)}(\mu_i) \quad (11)$$

$$K_i \cdot \frac{\Delta_i}{6} \cdot D_{i-1} + (K_i \cdot \frac{\Delta_i}{3} + \frac{\Delta_{i+1}}{3} \cdot K_{i+1}) D_i + K_{i+1} \cdot \frac{\Delta_{i+1}}{6} \cdot D_{i+1}$$

$$= (\frac{-K_i}{\Delta_i} - \frac{-K_{i+1}}{\Delta_{i+1}}) T_i + \frac{K_i \cdot T_{i-1}}{\Delta_i} + \frac{K_{i+1} \cdot T_{i+1}}{\Delta_{i+1}}, \text{ for } i=1(1)N-1 \quad (12)$$

Also from (6) and (9) we have following equation,

$$\frac{-\Delta_i}{6} D_{i-1} - \frac{\Delta_i}{3} D_i - (\frac{1}{\Delta_i} + \frac{h}{K_i}) T_i + \frac{T_{i-1}}{\Delta_i} + \frac{(hT_a - LE)}{K_i} = 0,$$

for $i=N$. (13)

From (5) and (8) we have

$$D_i + \frac{M_i}{K_i} (\sigma_1^{(i)} - 1) A_1^{(i)} \cdot T_i + \frac{M_i}{K_i} \cdot \sigma_2^{(i)} \cdot A_1^{(i)} \cdot T_0 + \frac{S_i}{K_i} \cdot A_1^{(i)} + \frac{\partial^2 T_i}{\partial \nu^2} = 0$$

Where $i=0(1)N$ (14)

Now (12), (13) and (14) can be written as,

$$P'_i \cdot D_i + P'_{i+1} \cdot D_{i+1} + P''_{i-1} \cdot D_{i-1} + Q'_{i+1} \cdot T_{i+1}$$

$$+ Q'_i \cdot T_i + Q''_{i-1} \cdot T_{i-1} + R''_i = 0 \quad \text{for } i=1(1)N-1 \quad (15)$$

$$P'_{i-1} \cdot D_{i-1} + P''_i \cdot D_i + Q''_i + Q'_{i-1} \cdot T_{i-1} + R'_i = 0$$

for $i=N$ only (16)

$$P_i \cdot D_i + P_{i-1} \cdot D_{i-1} + Q_i \cdot T_i + Q_0 \cdot T_0 + R_i + \frac{\partial^2 T_i}{\partial \nu^2} = 0$$

for $i=1(1)N$ (17)

Here, values of $P_i, P'_i, P'_{i-1}, P_{i+1}, P_{i-1}, P''_i, P''_{i-1}, Q_0, Q_i, Q'_i, Q''_i, Q_{i-1}, Q_{i+1}, Q''_{i-1}, R_i, R'_i$, and R''_i etc. are given in appendix.

Now, following *Fourier series* is applied to eliminate the variable ν from above equation (17). We have:

$$T_0 = A_{00} + \sum_{n=1}^{\infty} (A_{n0} \cdot \cos n\nu + B_{n0} \cdot \sin n\nu) \quad (18)$$

$$T_i = A_{0i} + \sum_{n=1}^{\infty} (A_{ni} \cdot \cos n\nu + B_{ni} \cdot \sin n\nu) \quad (19)$$

$$D_0 = \bar{A}_{00} + \sum_{n=1}^{\infty} (\bar{A}_{n0} \cdot \cos n\nu + \bar{B}_{n0} \cdot \sin n\nu) \quad (20)$$

$$D_i = \bar{A}_{0i} + \sum_{n=1}^{\infty} (\bar{A}_{ni} \cdot \cos n\nu + \bar{B}_{ni} \cdot \sin n\nu) \quad (21)$$

Here the coefficients A_{00}, A_{n0} , and B_{n0} are known due to boundary condition (4). All the coefficients $A_{0i}, \bar{A}_{0i}, \bar{A}_{00}, \bar{A}_{n0}, A_{ni}, \bar{A}_{ni}, B_{ni}, \bar{B}_{n0}$, and \bar{B}_{ni} ($i=1, \dots, N$) are unknowns and are obtained by solving the system of linear equations (15), (16), (17) and (18).

Here as a special case a dermal (SST) region of *elliptical organs resembling human limbs* have been considered. The SST region consists of three component layers namely *epidermis, dermis* and *subcutaneous tissues*. Thus the annular cross section of human limb has been divided into three annular layers (i.e. $N=3$). These three layers have different biological properties. The outermost layer epidermis is made up of mainly dead tissues. Hence it does not have any metabolic heat generation and blood flow. Below the epidermis is dermis, which consists of connective tissues, capillaries, sweat glands and fat cells etc. (Fig.1). The subcutaneous tissue consists of connective tissues, arterioles, venules, fat cells, sweat glands, and oil glands etc. The innermost solid cross-section is the limb core which consists of muscles, major blood vessels and bone etc. Parabolic variation of temperatures along the inner boundary has been taken as given below (Saxena and Bindra [10]):

$$T_0 = F(\nu) = \frac{(\nu - \pi)(\nu - 2\pi)}{2\pi^2} \cdot T_\alpha + \frac{2\nu(\nu - 2\pi)}{(-2\pi^2)} \cdot T_\beta + \frac{\nu(\nu - \pi)}{2\pi^2} \cdot T_\alpha \quad (22)$$

Where T_α and T_β are temperatures at $\nu=0$ and $\nu=\pi$ respectively. Using $F(\nu)$ in terms of Fourier series, the constants A_{00}, A_{n0} and B_{n0} are determined and then substituted in the system of equations (15), (16), and (17). These equations are solved to find the values of A_{0i}, A_{ni} and B_{ni} which in turn are substituted in expression (19) to obtain T_i and temperature profiles for each subregion. A computer program in MATLAB 7.0 has been developed to compute numerical results.

III. NUMERICAL RESULTS AND DISCUSSION

The following values of physical and physiological parameters have been used (Saxena and Bindra [10] and Pardasani and Adlakha[11]).

$$K_1 = 0.06 \text{ Cal/cm-min.deg.C}, K_2 = 0.045 \text{ Cal/cm-min.deg.C},$$

$$K_3 = 0.03 \text{ Cal/cm-min.deg.C}, L = 579.0 \text{ Cal/gm}, K_0 = K_1,$$

$$h = 0.009 \text{ Cal/cm}^2\text{-min.deg.C.}$$

The results have been computed for two cases of atmospheric temperatures and parameters M, S and E have been assigned the values as given below:

(i) $T_\alpha = 15^\circ \text{C}, E=0,$

$$M_1 = 0.003 \text{ Cal/cm}^3\text{-min.deg.C}, S_1 = 0.0357 \text{ Cal/cm}^3\text{-min.}$$

$$M_2 = 0.015 \text{ Cal/cm}^3\text{-min.deg.C}, S_2 = 0.0178 \text{ Cal/cm}^3\text{-min}$$

$$M_3 = 0, M_0 = M_1, S_3 = 0, S_0 = S_1, T_\alpha = 32^\circ \text{C and } T_\beta = 35^\circ \text{C}$$

(ii) $T_a = 23^0 C, E=0,$
 $M_1=0.018 Cal/cm^3-min.deg.C, S_1=0.018 Cal/cm^3-min.$
 $M_2=0.009 Cal/cm^3-min.deg.C, S_2=0.009 Cal/cm^3-min$
 $M_3=0, M_0=M_1, S_3=0, S_0=S_1, T_a=34^0C$ and $T_b=37^0C$

The constants μ_i ($i=0(1)3$) can be assigned any value depending upon the sample of skin layers under study. Here as particular case following values have been used

$\mu_0=6.0$ cm, $\mu_1=6.5$ cm, $\mu_2=6.9$ cm, $\mu_3=7.1$ cm. (jas [14]).

The expression for nodal information is as given below:

Angular Coordinates: -

$v_i = 0$ for $i=1(1)4,$ $v_{i+4} = v_i + 45^0$ for $i=1(1)28$

Radial Coordinates: -

$\mu_i = \mu_0$ for $i=1+4j, \mu_i = \mu_1, i=2+4j, \mu_i = \mu_2, i=3+4j, \mu_i = \mu_3, i=4+4j$
 for $j=0(1)7$

Eccentricity is given by: -

$d_i = d_1,$ for $i=2+4j,$
 $d_i = d_2,$ for $i=3+4j,$ for $j=0(1)7$
 $d_i = d_3,$ for $i=4+4j.$

The following eccentricities have been calculated for each layer.

$d_1=.0030$ $d_2=.0020$ $d_3=.0017$

The graphs have been plotted between T_i ($i=0(1)3$) and for two cases of atmospheric temperatures. Fig. 3 is for $T_a=15^0C$ and $E=0,$ and Fig. 4 is for $T_a=23^0C$ and $E=0.$

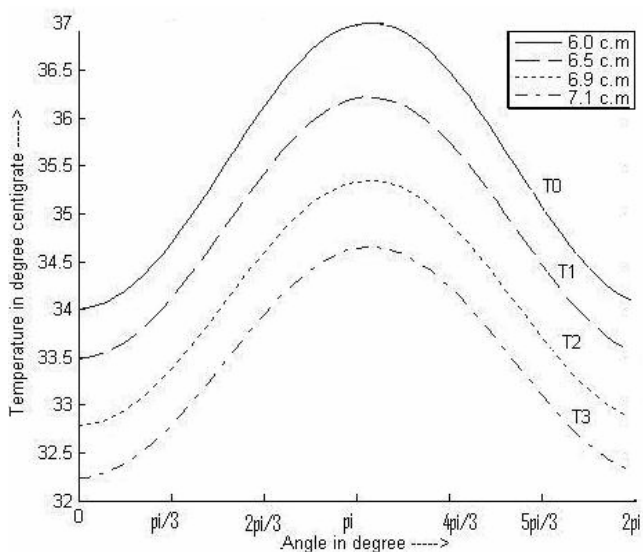


Fig. 3 Graph between Temperature T_i (0C) and angle v (deg.) for $T_a=15^0C$

The curve for T_0 in Fig.3 and Fig.4 are respectively the inner boundary conditions. The temperature rises slowly at $v=0$ and later on it rises sharply and takes on maximum at $v=\pi.$ There is significant difference among the curves with the increase in radial distances μ_i ($i=0(1)3$) from the centre. This may be due to heat loss from the outer surface to the environment. Thus the heat loss from the outer surface is quite significant. The variation in temperature is more for $T_a=15^0C$ in Fig. 3 as compared to Fig. 4 at $T_a=23^0C.$ This may be due to more heat loss to the environment at low atmospheric temperatures.

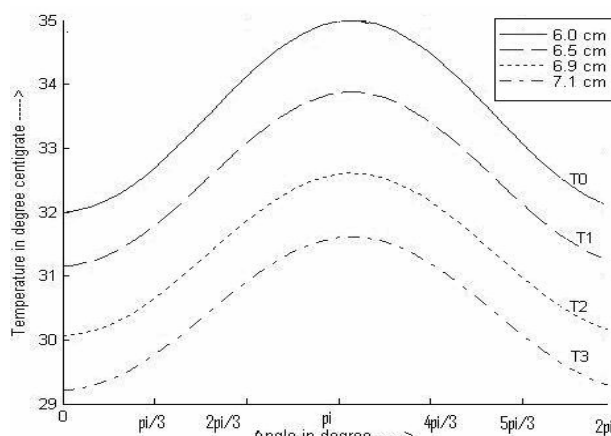


Fig. 4 Graph between Temperature T_i (0C) and angle v (deg.) for $T_a=23^0C$

The graphs in Fig.5 and Fig.6 represent the variation of temperature along radial direction for $T_a=15^0C$ and $T_a=23^0C$ respectively. In these figures it can be seen that the slope of the curve changes at the junction of each layer. This is due to different physiological properties of each layer. Also the temperature profiles fall downwards as we move towards the outer surface of the limb. This is due to the heat loss from the outer surface of the limb to the environment.

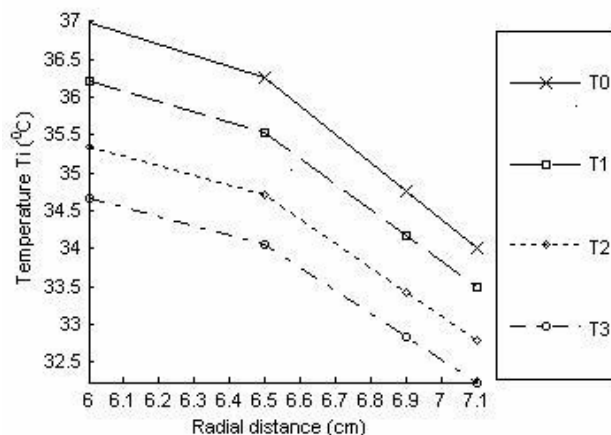


Fig. 5 Graph between Temperature T_i (0C) and Radial distance μ_i (cm) for $T_a=15^0C$

ACKNOWLEDGMENT

The authors acknowledge the Department of Biotechnology, New Delhi, India for providing the facility under Bioinformatics Infrastructural Facility for carrying out this work.

REFERENCES

- [1] W. Perl, "Heat and matter distribution in body tissues and determination of tissue blood flow by local clearance methods," *J.Theo. Biol.* 2, 201-235, (1962).
- [2] A. M. Patterson, "Measurement of temperature profiles in human skin," *S.Afr.J.Sc.* 72, 78-79, (1976).
- [3] V. P. Saxena, and D. Arya, "Steady state heat distribution in epidermis, dermis and subdermal tissues," *Theo. Biol.* 89, 423-432, (1981).
- [4] V. P. Saxena, and J. S. Bindra, "Indian J. pure appl.Math.," 18(9), 846-55, (1987).
- [5] K. R. Pardasani, and V. P. Saxena, "Bull. Calcutt Math.Soc." 81,1-8, (1989).
- [6] K. R. Pardasani, and N. Adlakha, "Coaxial circular sector elements to study radial and angular heat distribution problem in human limbs," *Proc. Nat. ACADE. Sci. India*, 68 (A), 1, (1998).
- [7] V. P. Saxena, and K. R. Pardasani, "Effect of dermal tumors on temperature distribution in skin with variable blood flow," *Mathematical Biology, USA*. Vol. 53, No.4, 525-536, (1991).
- [8] K. R. Pardasani, and N. Adlakha, "exact solution to a heat flow problem in peripheral tissue layers with a solid tumor in dermis," *Ind.J.Pure. Appl. Math.* 22 (8), 679-682, (1991).
- [9] J. W. Mitchell, T. L. Galvez, J. Hengle, G. E. Myers, and K. L. Siebecker, "Thermal response of human legs during cooling" *J.Appl. Physiology, U.S.A.*, 29 (6), 859-865, (1970).
- [10] V. P. Saxena, and J. S. Bindra, "Pseudo-analytic finite partition approach to temperature distribution problem in human limbs," *Int. J. Math. Sciences*. Vol. 12, 403-408, (1989).
- [11] K. R. Pardasani, and N. Adlakha, "Two-dimensional steady state temperature distribution in annular tissue layers of a human or animal body," *Ind.J.Pure. Appl. Math.* 24(11) 721-728, (1993).
- [12] M. K. Jain, S. Iyengar, and R. K. Jain, "Numerical Methods for Scientific and engineering Computation," Wiley Eastern Limited, (1985).
- [13] V. P. Saxena., and M. P. Gupta, "Steady state heat migration in radial and angular direction of human limbs," *Ind. J. Pure. Appl. Math.* 22(8), 657-668, (1991).
- [14] P. Jas, "Finite element approach to the thermal study of malignancies in cylindrical human organs," Ph.D. thesis, MANIT, Bhopal, (2002).
- [15] K. R. Pardasani, and M. Shakya, "Three dimensional infinite element model to study thermal disturbances in human peripheral region due to tumor" *J. of Biomechanics*, Vol. 39, Suppl.1, P.S634, (2006).
- [16] K. R. Pardasani, and M. Shakya, "Infinite element thermal model for human dermal regions with tumors." *Int. Journal of Applied Sc. & computations*, vol. 15 No., PP. 1-10, 1 May 2008.

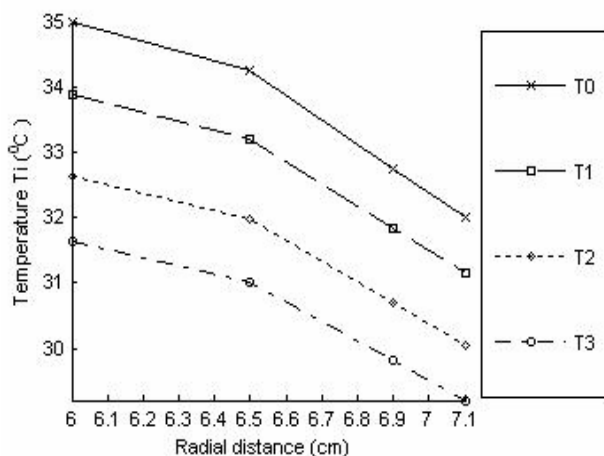


Fig. 6 Graph between Temperature T_i ($^{\circ}$ C) and Radial distance μ_i (cm) for $T_a = 23^{\circ}$ C

The computations involved in this method are less as compared to those in variational finite element method for a two dimensional steady case. Further the use of cubic splines along with Fourier series has given better accuracy and reduced the computations as compared with Ritz method along with Fourier series using linear shape and quadratic shape functions. Such mathematical models and techniques can be developed to study heat flow problems of human and animal body organs under various conditions and the information extracted from these models may prove to be useful for clinical situations like applications in thermography and hyperthermia.

APPENDIX

The values of constants used in equations (15), (16), and (17) are given as:

$$P_i = 1, P_{i-1} = 0, P'_{i-1} = \frac{-\Delta_i}{6}, k_{i+1} \cdot \frac{\Delta_{i+1}}{6}, Q_{i-1} = \frac{1}{\Delta_i}$$

$$P''_{i-1} = k_i \cdot \frac{\Delta_i}{6}, P'_i = (k_i \cdot \frac{\Delta_i}{3} + k_{i+1} \cdot \frac{\Delta_{i+1}}{3}), Q_i = \frac{M_i}{k_j} (\sigma_1^{(i)} - 1) L_1^{(i)}$$

$$Q_0 = \frac{M_i}{k_j} \cdot \sigma_2^{(i)} \cdot L_1^{(i)}, Q''_i = -(\frac{1}{\Delta_i} + \frac{h}{k_i}), Q_{i+1} = -\frac{k_{i+1}}{\Delta_{i+1}}, R''_i = 0$$

$$R_i = \frac{S_i}{k_j} \cdot L_1^{(i)}, Q'_i = (\frac{k_i}{\Delta_i} + \frac{k_{i+1}}{\Delta_{i+1}}), Q''_{i-1} = \frac{-k_i}{\Delta_i}, \text{ and}$$

$$R'_i = \frac{1}{k_i} (h \cdot T_a - L \cdot E).$$